JOURNAL OF THE SOUTHEASTERN ASSOCIATION FOR RESEARCH IN ASTRONOMY, **2**, 30-34, 2008 MAY 1

VII ZW 403, STRUCTURE RESOLVED IN A BLUE COMPACT DWARF GALAXY

TRISHA ASHLEY [1]
Department of Physics, Bryn Mawr College, Bryn Mawr, PA 19010

AND

CAROLINE SIMPSON
Department of Physics, Florida International University, Miami, FL 33199

ABSTRACT

VII Zw 403 is a blue compact dwarf galaxy, with one unresolved x-ray source. The galaxy was previously observed with the Very Large Array Radio Telescope in Socorro, New Mexico while in the C and D configurations; the data being analyzed in this paper are from the B-configuration. With these data, we have found some previously unresolved structure in the atomic hydrogen (H I) around an X-ray point source and other regions of the galaxy because of the higher resolution offered by the B-configuration. We are also able to see two differently oriented axes of rotation in the galaxy when the B, C, and D data are combined. One question that still needs to be explored is whether or not the x-ray source is the cause of some or all of the hole-like structure in the northeast section of the H I of the galaxy. This work may also shed light on how blue compact dwarf galaxies undergo starbursts without an obvious instigator.

Subject headings: galaxies: dwarf–galaxies: individual (VII Zw 403)–galaxies: ISM

1. INTRODUCTION

VII Zw 403 is a type of galaxy named for its small size and mass: a dwarf galaxy. There are three main types of dwarfs: elliptical, irregular, and blue compact dwarfs. Elliptical dwarf galaxies have properties similar to regular elliptical galaxies (i.e. they have little to no gas, and contain old Population II stars) and are most likely to be found near spiral galaxies Simpson (1995); Elmegreen (1998). Irregular dwarf galaxies come in a wide range of sizes and shapes, and often, more than half of their mass is in patchy gas that is frequently spread out quite far from the center (Hunter & Gallagher 1986). VII Zw 403 is a blue compact dwarf. These dwarfs are bright and have very blue centers (low B-V color) that indicate a high rate of star formation (Simpson 1995). Many theories on the origin and evolution of these dwarf galaxies have been formulated, but there has been very little resolution of the issue.

One question of importance is: why are blue compact dwarfs (BCDs) going through such intense periods of global star formation (also called star-bursting)? If this question can be answered then we will know more about the star formation process. Star formation that occurs in spiral galaxies, like our own, is better understood: the galaxy's arms are gravitational density waves that collect large amounts of gas and dust and compress it, allowing the interstellar medium to become dense enough to form stars. Unlike spiral galaxies, blue compact dwarf galaxies do not have density waves propagating through them. Instead, blue compact dwarfs are more like small splotches of gas that suddenly, rapidly, and globally begin to form stars, with no obvious instigator of the star formation. It has been suggested that blue compact dwarfs may be forming stars due to collisions and interactions with other galaxies (see Brosch et al. (2004) for an overview of the literature). Others speculate that the cause of star formation in dwarfs is highly dependent upon UV emission from massive stars and nebula feedback from dying stars, contributing to the churning of the interstellar medium (Hunter 1997). As no clear answer has yet emerged, the cause of these starbursting periods continues to be a well-researched topic.

2. PREVIOUS RESEARCH RESULTS FOR VII ZW 403

VII Zw 403 was previously observed at the Very Large Array (VLA)[2] in Socorro, NM, with the C and D configurations (Simpson et al. 2008). The D-configuration is the most compact configuration of the VLA. This creates a sensitive beam that has low resolution. The C-configuration is larger in extent (has longer baselines between antennas) so is less sensitive, but has better resolution. In both of these configurations, the galaxy's H I showed little structure and complicated velocity fields with some ordered rotation (Simpson et al. 2008).

In addition, Ott (2003) observed VII Zw 403 with the Chandra X-ray telescope. These observations showed one unresolved X-ray source and no diffuse X-ray emission. The unresolved source has a power-law spectral index resembling that of an X-ray binary (Ott 2003).

VII Zw 403 was also previously considered a member of the M81 galaxy cluster with a distance of 3.2 Mpc. Using high resolution data from the Hubble Space Telescope to find the luminosity of the tip of the red giant branch from color-magnitude diagrams, VII Zw 403's distance was determined to be 4.4 Mpc (Lynds et al. 1998). This puts it on the far side of the M81 group. It is still not known if the galaxy is a gravitationally bound member of the M81 group. However, it is clear that with a heliocentric velocity of approximately -100 km s^{-1}, VII Zw 403 is falling into the group. Whether it has already made previous journeys through the group is still undetermined.

3. OBSERVATIONS

The VLA was used to observe the H I emission from VII Zw 403. Twenty-one centimeter hydrogen line emission (H I

[1] Southeastern Association for Research in Astronomy (SARA) NSF-REU Summer Intern
Electronic address: tashley@brynmawr.edu; simpsonc@galaxy.fi u.edu

[2] The VLA is a facility of the National Radio Astronomy Observatory, operated by Associated Universities, Inc., under cooperative agreement with the National Science Foundation

TABLE 1
VLA OBSERVATIONS

Parameter	B configuration	B_N configuration[a]	B_{-1} configuration[b]
Observation Date	2006 Sept. 10	···	···
Time on Source (min)	542	···	···
Bandwidth (MHz)	1.56	···	···
No. of Channels	128	···	···
Velocity Resolution (km s^{-1})	2.6	···	···
Robustness Factor	···	···	-1
Beam Size ($''$)	···	5.48×5.27	3.69×3.53
Single channel r.m.s. (mJy $beam^{-1}$)	···	0.8	1.05

[a]Naturally weighted B-configuration data
[b]Uniformly weighted B-configuration data with ROBUST = –1

emission) takes place when excited hydrogen decays via the spin-flip transition into the lowest energy state, emitting a photon with the wavelength of 21cm. Although this transition is forbidden, the large amounts of atomic hydrogen in galaxies makes this spectral line observable. The areas where this occurs are reservoirs of H I which are potential areas for star formation.

Three of the VLA's configurations have been used to observe the galaxy's H I emission. The data analyzed in this paper was from the B configuration, which has a lower sensitivity but better resolution ($\sim 4''$) than the C ($\sim 12.5''$) and D ($\sim 1'$) configurations (Ulvestad et al. 2007). The B configuration source data was collected on September, 10th 2006 for approximately nine hours. The observations used 128 channels and on-line Hanning smoothing. The bandwidth was $\sim$1.56 MHz with channel separations of $\sim$12 kHz. The systemic velocity of this galaxy is roughly –100 km s^{-1}; the central frequency of the bandwidth was set to –64 km s^{-1} in order to match the C and D configuration data. Observational and data reduction parameters are given in Table 1.

In addition to H I observations made by the VLA, VII Zw 403 was observed at the Lowell Observatory with the Perkins 1.8m telescope to obtain UBVJ images. The UBV band images were made in March and April of 1999. The J band images were made in 1996 using the Ohio State Infrared Imager-Spectrograph (OSIRIS). Ionized hydrogen was also detected in VII Zw 403, using the Lowell Observatory. The Ohio State University Fabry-Perot was used in 1995 to help obtain the Hα images (Simpson et al. 2008). When there are very hot, very massive stars in an area of space, the stars radiate UV which then ionizes the surrounding hydrogen. The transition being detected occurs during recombination, when a photon of 6563 angstroms (656.3 nanometers) is emitted. This is called an Hα photon.

4. DATA REDUCTION

In previous analysis of the data from the C and D configurations, there has been a problem with galactic interference from the Milky Way. The Galactic interference was located at heliocentric velocities of 0 km s^{-1} and $\sim 55-80$ km s^{-1} (Simpson et al. 2008). In the B configuration data, the Galactic interference previously seen in the C and D configurations was unnoticeable; it was presumably at a scale that was too large for the longer baselines of the B configuration to resolve.

Data editing and calibration were done using standard routines in Astronomical Image Processing System (AIPS). We looked for interference and other problems using graphical (UVPLT) and TV-based (TVFLG) routines. Antennas 13, 14, 16, and 18 were flagged as bad antennas during the data collection process due to Extended Very Large Array testing errors and antennas 23, 24, 26, and 29 were not in use at the time.

The two calibrators for VII Zw 403 were a flux calibrator, 0134+329 (B1950), and a phase calibrator, 1436+763 (B1950). With SETJY in AIPS, we calculated the flux for 0134+329 to be 15.874 Jy. After running VLACALIB, several large phase jumps in the phase calibrator data, on the order of 100 degrees, were observed for some of the antennas. There were twelve of these large phase jumps in the right polarization data and eleven in the left.[3] All of these jumps occurred between scans near the end of the observing time. We reran the calibration using a different reference antenna in CALIB, understanding that the antenna we first chose may have been unstable or there may have been an isolated case of weather problems. Changing the reference antenna did not change the number or magnitude of the problematic jumps. After further consideration and testing, the galaxy source data from the scans that were in between the calibrator scans with phase jumps larger than 40 degrees were removed by flagging in TVFLAG. Careful examination of the resulting images (see below) revealed no artifacts that would indicate phase errors with the data. We also tried using self-calibration on the data, but the resulting images were essentially identical to those from the edited data. Results here are from the edited data that were not self-calibrated.

The AIPS task IMAGR was used to image and CLEAN the data, producing a cube of image channels, one for each frequency observed. The images were cleaned to a level of about 1σ (one times the r.m.s. value of a single channel). Different weighting options were used in order produce higher and lower resolution images. The natural weighting option produces a larger synthesized beam area, so has lower resolution but higher sensitivity (lower noise). Uniform weighting produces a smaller beam that can be adjusted according to a scale called ROBUST that runs from -5 to 5. The larger the ROBUST the larger the beam and the better the sensitivity, the smaller the ROBUST the smaller the beam and the better the resolution. The task MOMNT was then used with the resulting image cubes, integrating the signal in the channels without integrating the noise. The three images created by MOMNT are an H I map, a velocity map and a dispersion map.

[3] the polarization information is not used as H I emission is unpolarized; rather the two data independent data sets are combined during imaging to increase overall sensitivity

5. H I MORPHOLOGY

These new H I observations of VII Zw 403 have been able to resolve some interesting morphology within the galaxy. When the data were naturally weighted there were two clear peaks in density, one in the southern region and one in the northern region of the galaxy as can be seen in Figure 1.

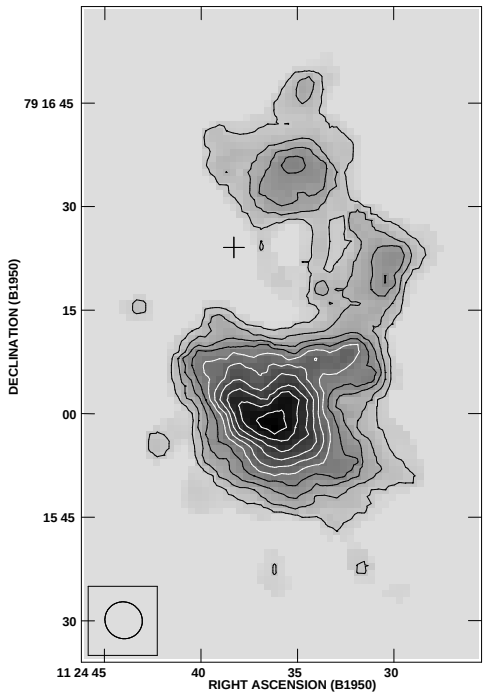

FIG. 1.— Integrated flux density map from the B-confi guration with natural weighting. The position of the X-ray source is marked with an X. The contour levels are (5, 10, 15, 20, 25, 30, 35, 40, 45 and 50)$\times 10^{20}$ atoms cm^{-2}.

The peak column density in the southern H I is 52.9×10^{20} atoms cm^{-2}. The northern H I reached a peak column density of 21.4×10^{20} atoms cm^{-2}. Right in between these two areas of high column density, there is an area in which the B-configuration was not sensitive enough to detect a great deal of signal, indicating that there are low H I gas levels in this area. This area of low density is surrounds the X-ray point source. This is consistent with the possibility that the X-ray point source is associated with a region of past star formation: if the point source is indeed an X-ray binary, perhaps it ionized or blew away some of the surrounding gas during the supernova explosion.

The naturally weighted H I contour plot with the Hα grey-scale shows Hα emission in both the middle and top sections of the southern high density H I region (see Figure 2). The V emission occurs in similar locations (see Figure 3). The difference between the V emission and the H α emission is that the V emission is also prominent not only in the southern region of the galaxy, but also in the low density area surrounding the X-ray source, indicating that there was star formation going on in these areas previously; and in the southern H I regions, there is continued star formation.

Even more structure in the galaxy's H I was visible in the uniformly weighted data of the galaxy with a ROBUST of −1 (refer to Figure 4). The southern region of high density is clearly composed of two different areas of high density with column densities of 41.6×10^{20} atoms cm^{-2} on the left and 39.9×10^{20} atoms cm^{-2} on the right.

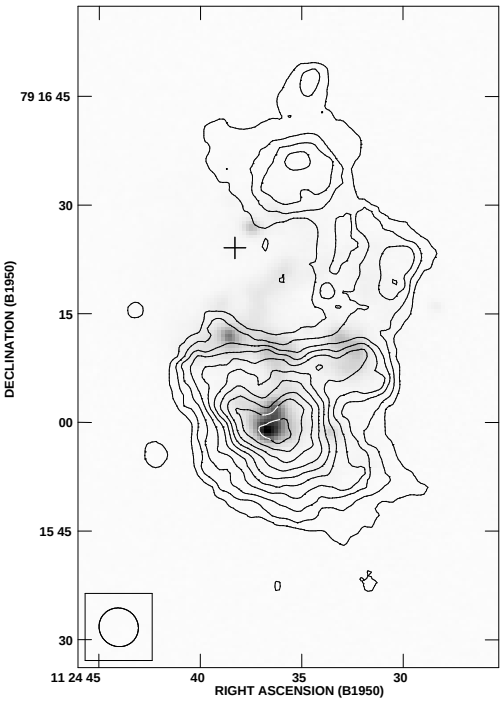

FIG. 2.— Hα emission in grey-scale with contours of the integrated flux density map from the B-confi guration data with natural weighting. The contour levels are (5, 10, 15, 20, 25, 30, 35, 40, 45 and 50)$\times 10^{20}$ atoms cm^{-2}.

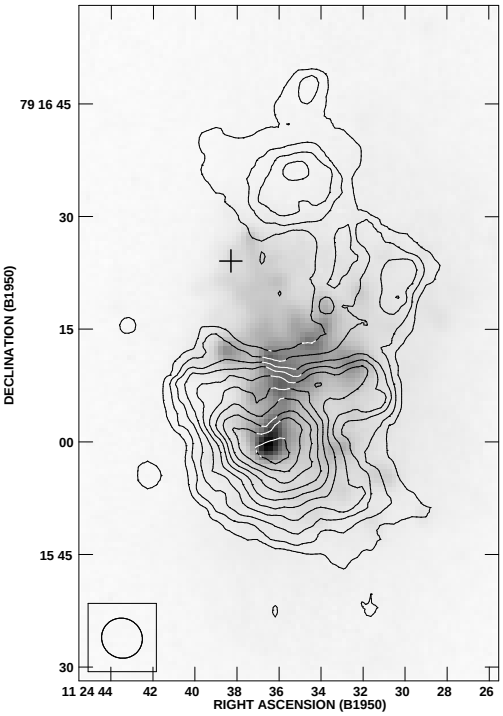

FIG. 3.— V-band emission in grey-scale with contours of the integrated flux density map from the B-confi guration with natural weighting. The contour levels are (5, 10, 15, 20, 25, 30, 35, 40, 45 and 50)$\times 10^{20}$ atoms cm^{-2}.

6. VELOCITY MAP

The velocity map from the naturally weighted B-configuration data is shown in Figure 5. The high resolution

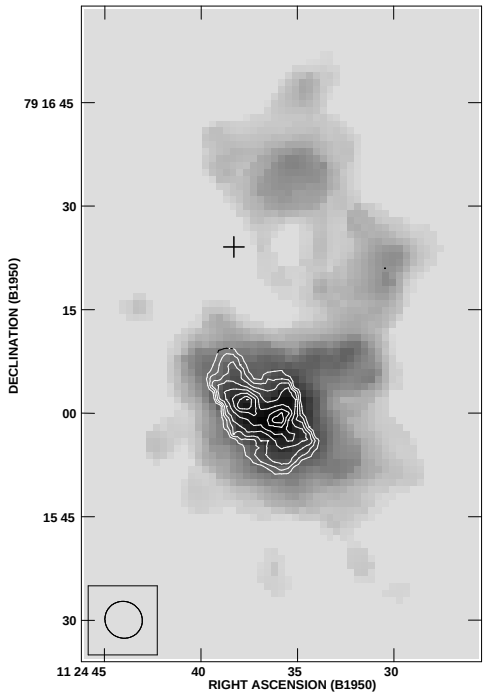

FIG. 4.— Integrated flux density map from the naturally weighted B-configuration data superimposed with the contours from the uniformly weighted B-configuration data at a ROBUST of −1. The contour levels are (1, 2, 3, 4, 5, 6, 7, 8, 9 and 10)×5.2×10^{20} atoms cm^{-2}.

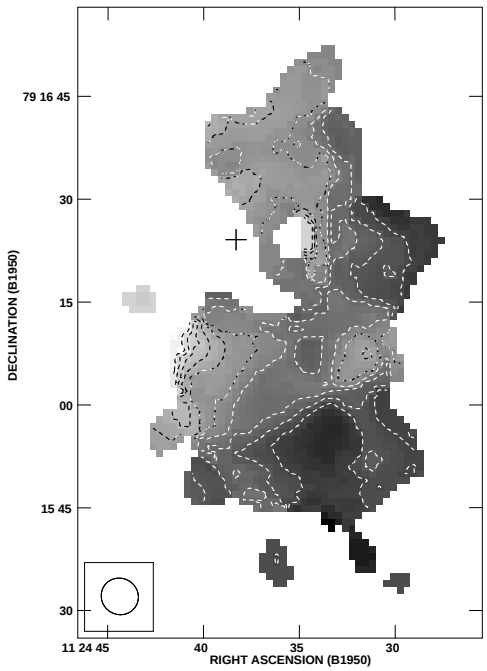

FIG. 5.— Velocity map from the naturally weighted B-configuration data. The contour levels are (-120, -117.5, -115, -112.5, -110, -107.5, -105, -102.5, -100, -97.5 and -95) with the lighter colors corresponding to more negative velocities (light = -120 km s^{-1}; dark = - 95 km s^{-1}).

of the B-configuration data emphasizes the smaller-scale (turbulent) motions in the gas, somewhat masking the larger-scale ordered (rotational) motions. In the southern velocities some structured rotation is visible; the receding gas is in the southwest end of the southern H I region and the approaching gas is to the north-east of the southern H I region. The peak velocity relative to the galaxy in the southern region is approximately 14 km s^{-1} and the minimum is approximately -20 km s^{-1}. The northern H I region of the velocity map is not as organized as the southern region.

In the previously combined C+D data, the H I in VII Zw 403 appears almost unstructured (refer to Figure 6 from Simpson et al. (2008)). With the higher resolution B data, the structure in the H I gas becomes very visible. We used DBCON to combine the B, C, and D configuration data (see Figure 7). IMAGR was run on the combined data set to image and clean it. For weighting, we used a ROBUST of 0, and -1, and we also made a full naturally weighted data set. After making sure the axes were in the correct order and units, the signal

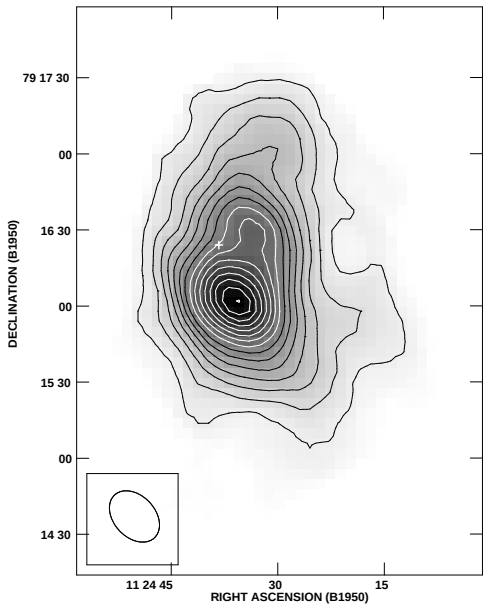

FIG. 6.— Integrated flux density map from the combined C+D configuration data. The contour levels are (2.5, 5, 7.5, 10, 12.5, 15, 17.5, 20, 22.5, 25, 27.5, 30, 32.5, 35 and 37.5) ×10^{20} atoms cm^{-2}.

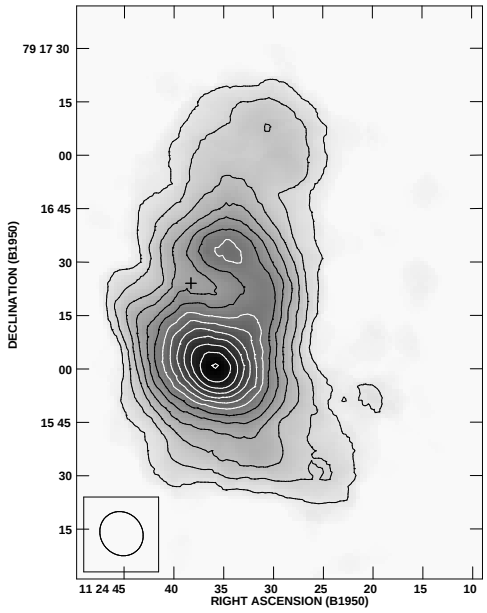

FIG. 7.— The B+C+D combined H I data with contour levels of (3.7, 7.3, 11, 14.7, 18.3, 22, 25.7, 29.4, 33, 36.7, 40.4, and 44) ×10^{20} atoms cm^{-2}.

was integrated up using MOMNT. The combined plots of the galaxy revealed the depression in H I around the X-ray source.

Another interesting attribute that the combined configurations displayed was in the velocity field seen in Figure 8.

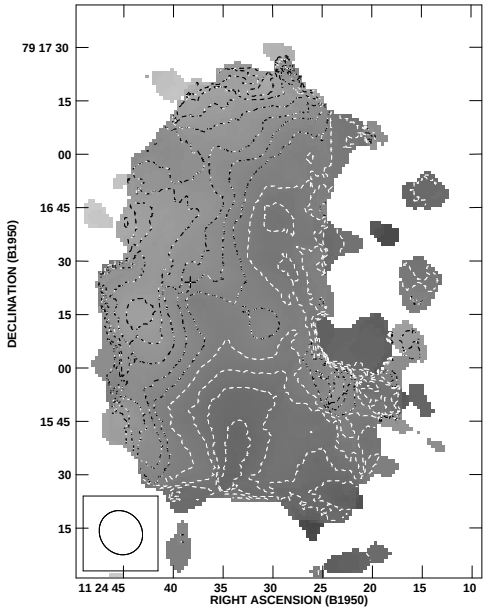

FIG. 8.— The B+C+D velocity map data with contour levels of -120, -117.5, -115, -112.5, -110, -107.5, -105, -102.5, -100, -97.5, -95) km s^{-1}.

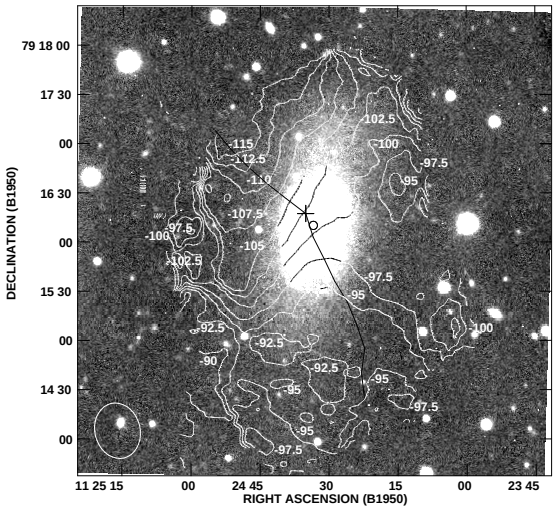

FIG. 9.— The combined C+D configuration data velocity contours on the V-band grey-scale. The white contours are labeled with the velocities of the galaxy in km s^{-1}. The black line represents the rotation axis from a rotation-curve fit (Simpson et al. 2008).

The general rotation of the galaxy is occurring in two separate sections: in the north and south areas of the galaxy, two separate rotation axes are seen. This is the break that was previously seen in the C+D velocity map shown in Figure 9.

7. CONCLUSIONS

The B-configuration data from the VLA allows us to see some structure in VII Zw 403 that was not previously resolved with the C and D configurations. The weak H I surrounding the X-ray source, the splitting of the high density regions of the galaxy into a northern and a southern region, and the existence of the two southern areas of high density, were all seen using information from the high resolution of the B-configuration. We were able to use this information and combine it with the original C and D configuration data to receive a more complete picture of the galaxy. The velocities of the gas became more obvious and the rotation axes of our galaxy became fairly noticeable. The drop in column density around the X-ray source is also obvious in the combined data. This is consistent with the effects of star formation on surrounding H I.

Areas of future work include calculating whether a supernova could have been energetic enough to form the depression in the H I we are seeing in the B-configuration data, and investigating what caused the star formation burst in the first place. If the galaxy is bound to the M81 cluster, it may have already passed through the cluster and is currently falling back in. A previous passage through the cluster and the resulting interactions with the cluster members or intra-cluster medium may have initiated the starburst if the timescales mesh. These questions are going to be researched at a later date.

This project was funded by a partnership between the National Science Foundation (NSF AST-0552798), Research Experiences for Undergraduates (REU), and the Department of Defense (DoD) ASSURE (Awards to Stimulate and Support Undergraduate Research Experiences) programs.

This work was partially funded by NSF grants AST-9802193 (July 1998-Dec 2001) and AST-0204922 (Sept 2002-Aug 2005) to D. A. Hunter and AST-9870112 (July 1998-June 2001) and AST-0205097 (Sept 2002-Aug 2005) to B. Elmegreen; and NSF AST-0407051 to C. E. Simpson.

We are also grateful to the following people for their support, aid, and knowledge:

Deirdre A. Hunter at the Lowell Observatory in Flagstaff, Arizona; Tyler Nordgren at the Department of Physics at the University of Redlands in Redlands California; Glenn Morrison with the Canada-France-Hawaii Telescope (CFHT) Corp. in Kamuela, Hawaii; Jurgen Ott at the National Radio Astronomy Observatory in Charlottesville, Virginia; and Michael Rupen and Frazer Owen at the National Radio Astronomy Observatory in Socorro, New Mexico.

REFERENCES

Brosch, N., Almoznino, E., & Heller, A. B. 2004, MNRAS, 349, 357
Elmegreen, D. M. 1998, Galaxies and Galactic Structure (New Jersey: Prentice Hall)
Hunter, D. A. 1997, PASP, 109, 937
Hunter, D. A., & Gallagher, J. S. 1986, PASP, 98, 5
Lynds, R., Tolstoy, E., O'Neil, E. J., & Hunter, D. A. 1998,AJ, 116, 146
Ott, J. 2003, PASP, 115, 141
Simpson, C. E. 1995, Ph.D. Thesis, University of Florida
Simpson, C. E., Hunter, D. A., & Nordgren, T. E. 2007, in preparation
Ulvestad, J. S., Perley, R. A., & Taylor, G. B. 2007, Observational Status Summary (www.vla.nrao.edu/astro)